Published OnlineFirst December 4, 2020; DOI: 10.1158/1535-7163.MCT-20-0464

Restoration of T-cell Effector Function, Depletion of Tregs, and Direct Killing of Tumor Cells: The Multiple Mechanisms of Action of a-TIGIT Antagonist Antibodies

Julie Preillon[1], Julia Cuende[1], Virginie Rabolli[1], Lucile Garnero[1], Marjorie Mercier[1], Noémie Wald[1], Angela Pappalardo[2], Sofie Denies[1], Diane Jamart[1], Anne-Catherine Michaux[1], Romain Pirson[1], Vincent Pitard[2], Martine Bagot[3], Shruthi Prasad[1], Erica Houthuys[1], Margreet Brouwer[1], Reece Marillier[1], Florence Lambolez[1], Joäo R. Marchante[1], Florence Nyawouame[1], Mathew J. Carter[4], Véronique Baron-Bodo[1], Anne Marie-Cardine[3], Mark Cragg[4], Julie Déchanet-Merville[2,5], Gregory Driessens[1], and Catherine Hoofd[1]

ABSTRACT

TIGIT is an immune checkpoint inhibitor expressed by effector $CD4^+$ and $CD8^+$ T cells, NK cells, and regulatory T cells (Tregs). Inhibition of TIGIT-ligand binding using antagonistic anti-TIGIT mAbs has shown *in vitro* potential to restore T-cell function and therapeutic efficacy in murine tumor models when combined with an anti–PD(L)-1 antibody. In the current work, we demonstrate broader TIGIT expression than previously reported in healthy donors and patients with cancer with expression on γδ T cells, particularly in CMV-seropositive donors, and on tumor cells from hematologic malignancies. Quantification of TIGIT density revealed tumor-infiltrating Tregs as the population expressing the highest receptor density. Consequently, the therapeutic potential of anti-TIGIT mAbs might be wider than the previously described anti–PD(L)-1-like restoration of αβ T-cell function. CD155 also mediated inhibition of γδ T cells, an immune population not previously described to be sensitive to TIGIT inhibition, which could be fully prevented via use of an antagonistic anti-TIGIT mAb (EOS-448). In PBMCs from patients with cancer, as well as in tumor-infiltrating lymphocytes from mice, the higher TIGIT expression in Tregs correlated with strong antibody-dependent killing and preferential depletion of this highly immunosuppressive population. Accordingly, the ADCC/ADCP–enabling format of the anti-TIGIT mAb had superior antitumor activity, which was dependent upon Fcγ receptor engagement. In addition, the anti-TIGIT mAb was able to induce direct killing of TIGIT-expressing tumor cells both in human patient material and in animal models, providing strong rationale for therapeutic intervention in hematologic malignancies. These findings reveal multiple therapeutic opportunities for anti-TIGIT mAbs in cancer therapeutics.

Introduction

TIGIT (T Cell Immunoreceptor With Ig And ITIM Domains) is a member of the poliovirus receptor (PVR)/*NECTIN* family and shares structural similarity with other immunoglobulin superfamily receptors (1). Cell-surface expression of TIGIT is mainly restricted to lymphocytes including effector $CD4^+$ and $CD8^+$ T and natural killer (NK) cells (2, 3). TIGIT is also constitutively expressed by regulatory T cells (Treg), where it is involved in regulating cellular homeostasis and function of this immunosuppressive T-cell subset (4).

TIGIT is bound by several ligands of the PVR/NECTIN family, with the highest affinity for CD155 (PVR), followed by CD112 (NECTIN-2 or PVRL2) and CD113 (NECTIN-3 or PVRL3; ref. 1). CD96 and CD112R (PVRIG) represent additional inhibitory receptors of the same family, which share common ligands and negatively modulate the effector functions of NK and T cells. CD226 (DNAM-1), in contrast, functions as a costimulatory receptor and shares CD155 and CD112 ligands with TIGIT. The pattern of expression of TIGIT and CD226 is analogous to that of cytotoxic T lymphocyte–associated antigen-4 (CTLA-4) and CD28. CD226 is expressed on naïve T cells, whereas TIGIT expression is upregulated upon activation or inflammatory stimuli (3, 5, 6). TIGIT elicits immunosuppression through several mechanisms, including the following: direct ITIM-mediated negative signaling; competition between TIGIT and CD226 for ligand binding that display higher affinities for TIGIT; enhanced IL10 and reduced IL12 production by dendritic cells (DC) after ligation of TIGIT on CD155 expressed at their surface, leading to a tolerogenic DC phenotype; and direct disruption of costimulatory signaling mediated by CD226 due to heterodimerization of TIGIT with CD226 (1, 3, 7, 8). In the context of chronic viral infection, $TIGIT^+$ T cells were demonstrated to have impaired effector function relative to their $TIGIT^-$ counterparts (9). Conversely, $TIGIT^+$ Treg cells are more effective at suppressing effector T-cell activation than their $TIGIT^-$ counterparts (10, 11) and are more efficient at inhibiting Th1 and Th17 responses (2).

[1]iTeos Therapeutics, Gosselies, Belgium and Cambridge, Massachusetts. [2]ImmunoConcEpT, UMR 5164, Bordeaux University, CNRS, Bordeaux, France. [3]INSERM U976, Université de Paris, Hôpital Saint Louis, Paris, France. [4]Antibody & Vaccine Group, Centre for Cancer Immunology, Cancer Sciences Unit, Southampton University Faculty of Medicine, Southampton, United Kingdom. [5]Team labeled LIGUE 2017.

Note: Supplementary data for this article are available at Molecular Cancer Therapeutics Online (http://mct.aacrjournals.org/).

J. Preillon, J. Cuende, V. Rabolli, G. Driessens, and C. Hoofd contributed equally to this article.

Corresponding Author: Gregory Driessens, Rue des Frères Wright 29, Gosselies 6041, Belgium. Phone: 327-191-9962; E-mail: gregory.driessens@iteostherapeutics.com

Mol Cancer Ther 2021;20:121–31

doi: 10.1158/1535-7163.MCT-20-0464

Published OnlineFirst December 4, 2020; DOI: 10.1158/1535-7163.MCT-20-0464

TIGIT expression has been observed to be upregulated in human tumors (3), with higher expression on tumor-infiltrating lymphocytes (TIL) compared with circulating peripheral blood mononuclear cells (PBMC) or immune cells from tumor-adjacent tissue in patients with liver cancer (12). Similarly, a higher proportion of $TIGIT^+$ $CD4^+$ T cells was observed in skin and PBMCs from cutaneous T-cell lymphoma (CTCL) patients than from healthy donors (13). In summary, high TIGIT expression on intratumoral T has been described in a wide range of both solid tumors and blood cancers and associated with dysfunctional $CD8^+$ T cells (recently reviewed in ref. 14).

Because TIGIT ligands are highly expressed on tumor cells in a wide array of cancers (15), interaction with $TIGIT^+$ TILs represents a common mechanism to create an immunosuppressive tumor microenvironment (TME) for infiltrating T and NK cells. Consequently, TIGIT is a relevant target of interest for cancer immunotherapy (16), as supported by preclinical studies and recent communication on the clinical efficacy of anti-TIGIT Ab tiragolumab developed by Roche. Pharmacologic blockade of TIGIT with an antagonistic antibody inhibits tumor growth in murine tumor models either alone or in combination with immune checkpoint inhibitors (ICI), such as anti–PD-1 or anti–PD-L1 antibodies (3, 17–21). The degree of antitumor response depends on the isotype of the antagonistic anti-TIGIT mAb and whether CD155 ligand can engage CD226, because efficacy is lost if CD226 is simultaneously blocked (3). Furthermore, *ex vivo* antigen-specific restimulation of T cells from vaccinated patients with cancer demonstrated the ability of anti-TIGIT mAb alone or in combination with anti–PD-1 to increase the effector functions of T cells targeting tumor antigens (22). On the basis of these findings, several anti-TIGIT Abs in various forms, such as IgG1, IgG1 variant with low affinity to Fcγ receptors (FcγR), and IgG4, are currently being tested in phase I and phase II clinical trials (23).

These observations led us to investigate the potential for therapeutic intervention with anti-TIGIT mAb, and, to the best of our knowledge, this is the first report to show that, in addition to the well-described PD (L)-1–like activity to restore αβ T-cell function, anti-TIGIT mAb therapy increases the function of γδ T cells isolated from healthy donors. Depending on the isotype, an anti-TIGIT mAb also mediated direct killing of tumor cells and immunosuppressive Tregs both in cancer patient samples and preclinical mouse models. This latter activity was dependent upon engaging activatory FcγR. These findings reveal novel immunosuppressive mechanisms of TIGIT in cancer and broader therapeutic opportunities for anti-TIGIT drugs. They also support the selection of anti-TIGIT mAbs with good affinity for activatory FcγR as the format of drug with the greatest therapeutic potential for patients with cancer.

Materials and Methods

Tumor microarray and fresh tumor dissociation

A total of 21 formalin-fixed paraffin-embedded (FFPE) disease-specific tissue microarray (TMA) blocks were assembled with primary tumors from nine cancer types (13–51 donors per cancer type) from patients with different histotypes and different disease stages at Institut de Pathologie et de Génétique (IPG; Gosselies, Belgium). The research project was approved by Jules Bordet Ethical Committee (#CE2797). Sections of colon cancer TMA (64 cores derived from 64 colon adenocarcinoma cancer patients) were purchased from Biochain (#T8235722–5).

Tumors, which were surgically removed after informed consent was obtained, were collected by BioPartners. Resections were placed directly in cold AQIX RS-I media (AQIX) for transport and, immediately after arrival (within 28 hours after surgery), were minced with scalpels and dissociated using the Tumor Dissociation Kit and the GentleMax Dissociator (Miltenyi Biotec). Single-cell suspensions were obtained by pooling two successive dissociation rounds and filtering through a 70-μm nylon mesh cell strainer.

PBMCs and T-cell isolation

Blood samples from patients with cancer were collected by BioPartners on the day of tumor resection. Venous blood samples from healthy volunteers (approved by the Ethics Committee, FOR-UIC-BV-050–01–01 ICF_HBS_HD Version 7.1) were obtained from Tivoli Hospital (La Louvière, Belgium). PBMCs were isolated by lymphoprep density gradient centrifugation used in combination with SepMate (Stemcell Technologies) tubes according to the manufacturer's instructions. After purification, cells were immediately characterized by flow cytometry or frozen in 90% FBS and 10% DMSO in liquid nitrogen. $CD8^+$ T cells were purified from frozen human PBMCs using negative selection (Stemcell Technologies) according to the manufacturer's recommendations.

Flow cytometry

PBMCs or dissociated tumor cells (DTC) were stained per the manufacturer's instructions using filtered PBS, 2 mmol/L EDTA, 0.1% BSA FACS buffer, and Brilliant Stain buffer (BD Biosciences). Cells were blocked with Human FcBlock for 10 minutes at room temperature before incubation for 20 minutes at 4°C with antibody cocktail, as specified in Supplementary Table S1. Cells were washed twice and fixed using BD Cell Fix buffer prior to acquisition. Viable single cells were gated on Forward and Side scatter and using fixable viability dye (FVD) efluor780.

For *ex vivo* stimulated samples, PBMCs were suspended in X-vivo15 medium (Westburg) and activated as described previously (24).

Cell samples were analyzed using a 4-laser LSR Fortessa flow cytometer (BD Biosciences) using Diva software and analyzed with FlowJo software v10.6.1 (FlowJo).

CD155, pan-cytokeratin, and CD226 staining by IHC

CD155, pan-cytokeratin (PanCK), and CD226 staining of multiple cancer TMAs was performed according to methods described in the Supplementary Materials.

Coculture of CD155-expressing cells and $CD8^+$ T cells

CD155 APC/CHO-K1 (Promega) cells were incubated at 37°C and 5% CO_2 overnight according to the manufacturer's recommendations. Then, healthy donor $CD8^+$ T cells were incubated with increasing concentrations (0.011–333 nmol/L) of a fully human IgG1 anti-TIGIT Ab EOS-448 (iTeos Therapeutics) and were added to CD155 APC/CHO-K1 cells and incubated at 37°C and 5% CO_2 for 5 days. IFNγ concentrations were assessed in cell supernatants by ELISA (Affymetrix eBioscience). EOS-448 Ab corresponds to clone 31282 sequence in PCT application WO/2020/114178.

In vitro antibody-dependent cellular death assay in human PBMCs

Cryopreserved isolated PBMCs from healthy volunteers and patients with cancer were provided by ImmunXperts and ConversantBio, respectively. PBMCs were thawed, resuspended in RPMI medium supplemented with 10% FBS + 50 U/mL penicillin/streptomycin (Westburg), and incubated at 37°C and 5% CO_2 for 20 hours with anti-TIGIT EOS-448 (IgG1, iTeos Therapeutics), anti-TIGIT EOS026452 (hIgG1, IgG2, IgG4; iTeos Therapeutics) mAb, isotype

control (Bio X Cell), or rituximab at a final concentration of 6.6 nmol/L. Cells were then stained for surface markers, as indicated in Supplementary Table S1. After washing, cells were fixed and, immediately before acquisition, AccuCheck Counting beads (Thermo Fisher Scientific) were added for absolute quantification of each cell type/μL following the manufacturer's specifications. Data were acquired as described for flow cytometry. The absolute number of cells per μL was calculated for different T- and B-cell populations after exclusion of FVD^+ cells. The percentage of specific lysis was calculated using the following formula: $(1-(a/b)) \times 100$, where a is absolute cell counts/μL in a well incubated with either EOS-448 or rituximab, and b is the mean of the absolute cell counts/μL from triplicate wells treated with isotype antibody control.

γδ T-cell functional assay

PBMCs were obtained from the Etablissement Français du Sang Aquitaine Limousin blood bank and were isolated by gradient centrifugation and resuspended in RPMI supplemented with 10% FCS. PBMCs were cultured with IL15 (20 ng/mL) and MACS magnetically sorted Vδ1 γδ T cells. T cells were activated with 10 μg/mL anti-Vδ1 antibody (clone R9.12, Beckman Coulter). Recombinant human CD155-Fc (R&D Systems) was added at 10 μg/mL, with or without 66.6 nmol/L EOS-448. Cells were cultured for 48 hours at 37°C and 5% CO_2; supernatant was then collected and IFNγ concentration measured by ELISA (MabTech Kit). Production of Granzyme B, GM-CSF, and TNFα was assessed by Cytometric Bead Array (Flex Set CBA, BD Biosciences) per the manufacturer's recommendations.

Mice

Eight-week-old female BALB/c or C57BL/6 mice (Charles River Laboratories) were housed at the specific pathogen-free facility of the IMI, Gosselies, Belgium, in individually ventilated cages. All experiments were performed in accordance with national and institutional guidelines for animal care and the approval of the local Animal Ethics Committee. For experiments conducted in Southampton (United Kingdom), 8- to 12-week-old female BALB/c and Fc receptor gamma chain knock-out mice (FcR γ chain KO) were generated as described previously (25). Animal experiments were conducted according to the UK Home Office license guidelines and approved by the University of Southampton Ethics Committee. During the study, the care and use of animals were in accordance with the regulations of the Association for Assessment and Accreditation of Laboratory Animal Care.

Tumor growth and treatments in mice

A total of 5×10^5 CT26 (ATCC CRL-2638™), 1×10^6 EL4-mTIGIT, 0.2×10^6 EL4-GFP (both originating from EL4 purchased at ATCC TIB-39™), or 5×10^6 Hepa1–6 (CrownBio) tumor cells were inoculated subcutaneously in the right flank of BALB/c, C57BL/6, or activatory FcγR chain KO mice (25). Tumor volume was measured three times per week as described previously (24). For the pancreatic cancer model, 2×10^6 PanO2-Luc (originating from PanO2 cells, purchased at NCI 0507406) cells were resuspended in 50 μL of ice-cold Matrigel-RPMI medium (1:1) and orthotopically implanted in the tail of the pancreas. Tumor growth was monitored weekly by bioluminescent imaging performed at the Center for Microscopy and Molecular Imaging (CMMI, UMONS). All cell lines were grown upon receipt for 2 to 3 passages to generate a working stock. A new vial from the working stock was thawed to perform each individual *in vivo* experiment. Cells were cultured for a maximum of 2 weeks and regularly checked for *Mycoplasma* using MycoAlert Mycoplasma Detection Kit from Lonza

Because human anti-TIGIT mAb EOS-448 does not cross-react with mouse TIGIT, the anti-TIGIT antibody used in murine models is a surrogate antibody produced at UProtein. Mice were randomized when tumors were established and treated using PBS or mIgG2a isotype (200 μg/mouse, Bio X Cell BE0085), anti-TIGIT mIgG2a (20 or 200 μg/mouse), anti-TIGIT mIgG1 (200 μg/mouse), anti-TIGIT hIgG1 (200 μg/mouse), anti-TIGIT hIgG1-N297A (200 μg/mouse), anti–PD-1 (200 μg/mouse, Bio X Cell BE0146), anti-4-1BB (TNFRSF9; 5 μg/mouse, Bio X Cell BE0239), anti-OX-40 (TNFRSF4; 20 μg/mouse, Bio X Cell BE0031), or anti-GITR (TNFRSF18; 10 μg/mouse, Bio X Cell BE0063), as indicated for specific models. Anti-CD4 (250 μg/mouse, Bio X Cell BE0003–1) prophylactic treatment was performed at seven days and four days before tumor inoculation, then weekly until the end of the study. Some antibodies were combined, as indicated in the figure legends. All antibodies were diluted in PBS prior intraperitoneal injection every three days for a total of three to four injections.

Dissociation of murine tumors and spleens

Two days after the second anti-TIGIT treatment, CT26 tumor-bearing mice were sacrificed and eight tumors per group were collected in ice-cold PBS and dissociated using mouse Tumor Dissociation Kit from Miltenyi Biotec. Spleens were collected in ice-cold PBS and crushed through a 70-μm filter; cells were resuspended in red blood cell lysis buffer (Sigma) for four minutes. Splenocytes were resuspended in complete medium and processed for staining. Surface staining was performed as described in the Supplementary Materials.

Measurement of TIGIT expression and *ex vivo* ADCC assay in blood samples from patients with Sézary syndrome

Blood samples were obtained from patients with Sézary syndrome, a particular form of CTCL with circulating clonal $CD4^+$ tumor cells, after written informed consent was obtained and the protocol was approved by the institutional ethics committee (Saint Louis Hospital, Paris, France). To distinguish between tumor and normal $CD4^+$ T cells, predetermination of the malignant clone TCR-Vβ rearrangement was performed on peripheral blood (Beckman Coulter TCR-Vβ Repertoire Kit).

Only patients whose malignant clone could be identified through its TCR-Vβ rearrangement were processed for evaluation of TIGIT expression profile on immune cells. TIGIT expression was monitored in normal and malignant $CD4^+$ T, $CD8^+$ T, B, and NK cells by flow cytometry using antibodies described in Supplementary Table S1.

For the antibody-dependent cell-mediated cytotoxicity (ADCC) assay, patient samples were treated as described previously (26). Purified $CD4^+$ T cells were preincubated for 30 minutes at room temperature with an hIgG1, anti-TIGIT EOS-448, or positive control antibody corresponding to alemtuzumab sequence (produced at UProtein) at 66.6 nmol/L and then mixed with the autologous sorted NK lymphocytes at the indicated effector:target (E:T) ratios. Incubation was conducted for 4.5 hours at 37°C and 5% CO_2.

Statistical analyses

Statistical analyses were performed using GraphPad Prism version 7 and are described in the figure legends. Tumor growth curves were fitted with a linear mixed model using SAS JMP version 13 after log transformation of tumor volumes. Fixed effects included time and treatment. Polynomial functions of time were included based on significance of the polynomial term in sequential tests. The necessity to include random effects was assessed by a Wald test. Good model fit was assessed by plotting the fitted versus observed tumor growth

Published OnlineFirst December 4, 2020; DOI: 10.1158/1535-7163.MCT-20-0464

curves and by residual analysis. A treatment difference in tumor growth was tested by a joint hypothesis test for the interaction terms of time and treatment (27).

Results

Expression of TIGIT, CD226, and CD155 in patients with cancer and healthy volunteers

We first characterized the expression of the main targets of the TIGIT pathway in the TME in several solid cancer indications. The assessment of CD155 and CD226 by IHC in TMAs (Supplementary Fig. S1) showed a high CD155 expression by tumor cells in the 10 indications analyzed, especially in pancreas, prostate, and kidney cancers, where more than 20% of tumor cells (median value) were CD155^{high} (**Fig. 1A**). CD226 was mainly expressed by immune cells in the TME and was observed in the nine cancer types analyzed (**Fig. 1B**). To characterize TIGIT expression in different immune populations and explore its modulation in the tumor environment, we compared the proportion of TIGIT-expressing cells, as well as the number of TIGIT molecules per cell in PBMCs from healthy donors or matched PBMCs, with TILs from patients with cancer with multiple solid tumor indications by flow cytometry (Supplementary Fig. S2). We observed an increased proportion of TIGIT-expressing cells in the NK and T-cell populations analyzed (CD4$^+$, CD8$^+$, Tregs, NK, and NKT-like cells) in PBMCs from patients with cancer compared with those from healthy donors. TIGIT expression on TILs was further enhanced in non-Treg CD4$^+$, CD8$^+$, Tregs, and NKT-like cell populations, but not in NK cells. Infiltrating Tregs and CD8$^+$ T cells showed the highest frequency, with more than 85% TIGIT$^+$ cells (**Fig. 1C**). Interestingly, the number of TIGIT receptors per cell was also higher in PBMCs from patients with cancer than those from healthy donors in all tested immune populations. Although the number of receptors observed in PBMCs and TILs was similar for most populations, an additional 2-fold increase of TIGIT in Treg cells was observed in the tumors. As expected, non-T/NK-cell populations (CD45$^+$CD3$^-$CD56$^-$) had a very low level of TIGIT expression (**Fig. 1D**). Overall, TIGIT and CD226, as well as their ligand CD155, were highly expressed in the TME, with an increased proportion of TIGIT-expressing cells in TILs and the highest level of TIGIT in Tregs.

TIGIT-expressing TILs have impaired functionality that is reversed by anti-TIGIT mAb

To characterize and compare the functional activity of TIGIT$^+$ and TIGIT$^-$ T cells, we measured cytokine production after *ex vivo* stimulation of human TILs. In both CD4$^+$ and CD8$^+$ T-cell populations, the majority of TIGIT$^+$ cells were also expressing PD-1 and CD39, which was not the case for TIGIT$^-$ cells (Supplementary Fig. S2C). Functionally, TIGIT$^-$ T cells had a much higher proportion of IFNγ-, IL2-, or TNFα-expressing cells than TIGIT$^+$ cells, confirming that TIGIT-expressing TILs have a dysfunctional phenotype (**Fig. 2A**; Supplementary Fig. S2). Interestingly, this finding was restricted to TILs, compared with PBMCs where TIGIT$^+$ cells maintained their ability to produce TNFα or IFNγ after stimulation (**Fig. 2B**).

To test the potential of anti-TIGIT mAb EOS-448 to restore functional activity of TIGIT$^+$ cells, we first confirmed its ability to prevent CD155 binding and increase the functional activity of Jurkat cells that were engineered to overexpress TIGIT, as measured using a reporter assay (Supplementary Fig. S3). Next, we tested the effect of EOS-448 on CD8$^+$ T cells from healthy donor PBMCs activated in the presence of CD155-expressing cells and demonstrated that blocking TIGIT restored secretion of IFNγ in a dose-dependent manner

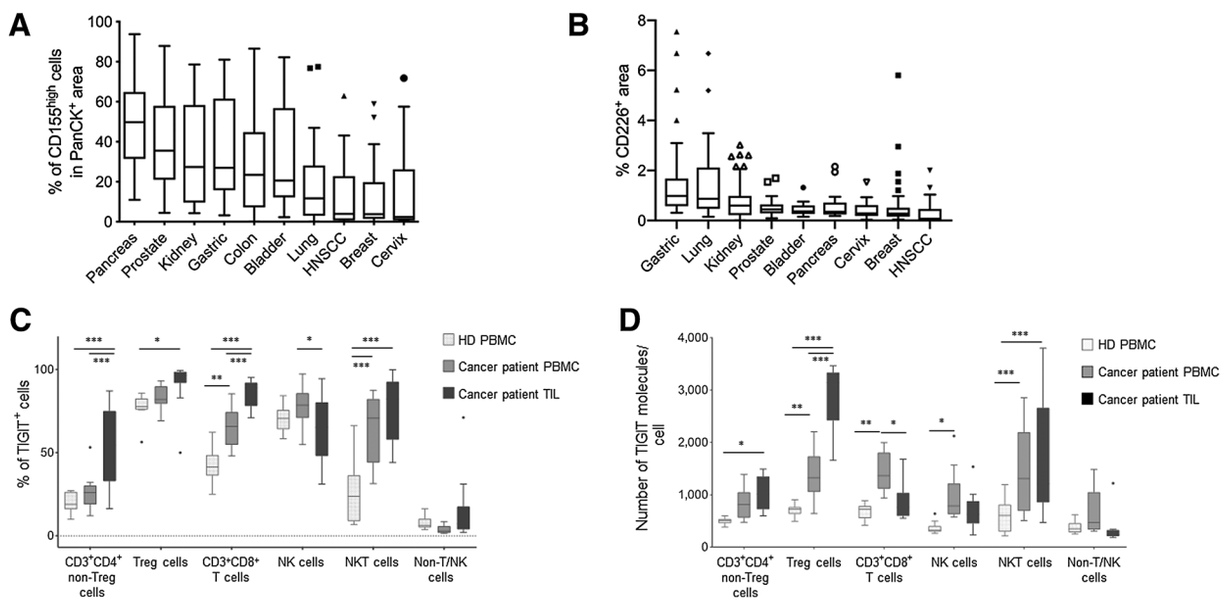

Figure 1.

CD155, CD226, and TIGIT are highly expressed in various solid cancers. **A,** Percentage of CD155^{high} cells analyzed within tumor area (pan-cytokeratin$^+$) after IHC staining of TMAs ($n = 284$ samples from 10 different indications). **B,** Percentage of CD226$^+$ tissue area ($n = 307$ tumor samples from nine different indications). **C** and **D,** Flow cytometry analysis of PBMCs from healthy donors ($n = 10$) matched PBMCs and dissociated tumor samples from different cancer indications ($n = 12$) showing the frequency of TIGIT-expressing cells on different immune subsets (**C**) or the number of TIGIT receptors expressed at the membrane (**D**). Data are represented as Tukey plots. *, $P < 0.05$; **, $P < 0.01$; ***, $P < 0.001$ by two-way ANOVA analysis with multiple comparisons.

Published OnlineFirst December 4, 2020; DOI: 10.1158/1535-7163.MCT-20-0464

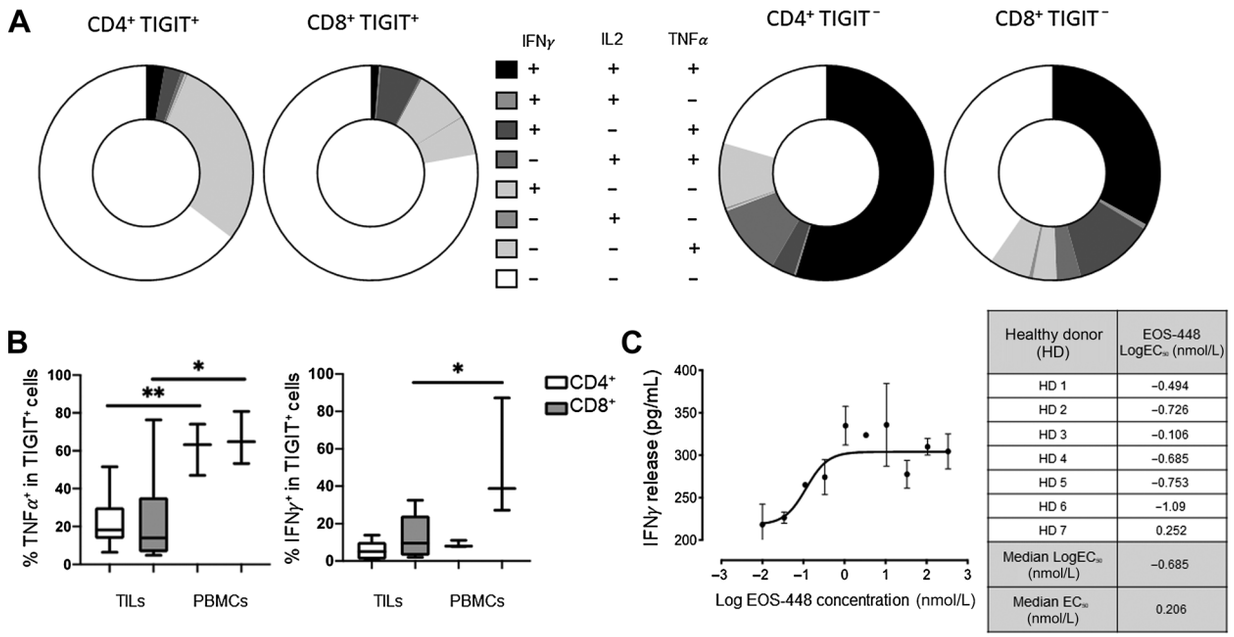

Healthy donor (HD)	EOS-448 LogEC$_{50}$ (nmol/L)
HD 1	−0.494
HD 2	−0.726
HD 3	−0.106
HD 4	−0.685
HD 5	−0.753
HD 6	−1.09
HD 7	0.252
Median LogEC$_{50}$ (nmol/L)	−0.685
Median EC$_{50}$ (nmol/L)	0.206

Figure 2.

TIGIT-expressing TILs are not functional, but T-cell activity can be restored by antagonist anti-TIGIT Ab. **A,** Donut plots representing the results of intracellular staining for cytokines in dissociated tumor cells from a patient with kidney cancer. Cells were stimulated for 3 hours with a mix of PMA/ionomycin in the presence of Monensin and Brefeldin A. Data represent multiple expression (Boolean gate) of the frequency for IFNγ, IL2, or TNFα among the TIGIT$^+$ or TIGIT$^-$ CD4$^+$ and CD8$^+$ TIL populations. **B,** Graphs representing FACS analysis of CD4$^+$ and CD8$^+$ T lymphocytes comparing isolated cancer PBMCs ($n = 1$ lung, $n = 1$ melanoma, and $n = 1$ RCC) and dissociated primary tumor cells ($n = 2$ breast, $n = 1$ lung, $n = 1$ melanoma, and $n = 1$ RCC) for the production of IFNγ or TNFα after stimulation. Data are represented as Tukey plots for frequency of IFNγ$^+$ and TNFα$^+$ cells among the TIGIT$^+$ T cells. *, $P < 0.05$; **, $P < 0.01$ by Student t test. **C,** Dose response curve and table for EC$_{50}$ values showing the activity of anti-TIGIT EOS-448 mAb to induce IFNγ release by CD8$^+$ T cells activated in the presence of CD155-expressing cells. Graph shows one representative experiment out of seven (means of IFNγ concentration ±SD).

(**Fig. 2C**). EOS-448 was also able to boost the functional activity of T cells in samples from solid tumor patients, although the activity of anti-TIGIT was donor dependent (Supplementary Fig. S3). These results showed that TIGIT$^+$ T cells from patients with cancer are dysfunctional and that TIGIT blockade has the potential to improve the function of immune cells in the periphery and in the TIGIT-rich TME.

CD155/TIGIT axis is immunosuppressive in γδ T cells and can be reverted by EOS-448

Immunosuppressive activity of TIGIT has been well described for αβ T cells, but nothing is known regarding its inhibitory function on nonconventional γδ T cells. We observed a high expression of TIGIT on γδ T cells that was higher than on NK or αβ T cells (**Fig. 3A**). γδ T cells can be divided into two populations according to expression of the Vδ2 chain of the TCR, with Vδ2$^+$ γδ T cells being phosphoantigen-responding and Vδ2$^-$ γδ T cells being cytomegalovirus (CMV)-responding (28). The percentages of TIGIT$^+$ cells and the intensity of TIGIT expression were higher among Vδ2$^-$ than Vδ2$^+$ γδ T cells (**Fig. 3A**). Of interest, Vδ2$^-$ γδ T cells from CMV-seropositive donors exhibited higher TIGIT expression than those from CMV-seronegative donors (**Fig. 3A**). Increased expression of TIGIT in CMV-seropositive donors was also seen for αβ T cells, whereas no difference was observed for NK cells or Vδ2$^+$ T cells (**Fig. 3A**). CMV seropositivity did not uniformly affect all inhibitory checkpoints, as shown by CMV serostatus having no influence on PD-1 expression on γδ T cells, whereas NK and αβ T cells had higher proportions of PD1$^+$ cells in CMV-seropositive samples (**Fig. 3B**). As previously observed for αβ T cells, the TIGIT$^+$ Vδ2$^-$ γδ T cells comprise mainly differentiated cells with cytotoxic potential, as characterized by their CD45RA$^+$ CD27$^-$ CD28$^-$ granzyme$^+$ phenotype (Supplementary Fig. S4). We next determined whether TIGIT expression could elicit immunosuppressive signaling in γδ T cells and if anti-TIGIT treatment could functionally restore activity of γδ T cells, as observed in αβ T cells (**Fig. 2**). We activated Vδ1 T cells within PBMCs from CMV$^+$ donors with an agonist anti-Vδ1 mAb in the presence of a soluble form of CD155 with and without anti-TIGIT mAb EOS-448. CD155 elicited a strong inhibitory effect on Vδ1 T-cell activation, as measured by a decrease of IFNγ secretion. The addition of anti-TIGIT mAb EOS-448 fully prevented CD155-mediated inhibition (**Fig. 3C**). This inhibitory effect, which was induced by CD155 and prevented by EOS-448, was not restricted to IFNγ, with a rescue observed for other proinflammatory cytokines (did not reach statistical significance; **Fig. 3D**). In conclusion, TIGIT is strongly expressed in γδ T cells, particularly in CMV-seropositive individuals who represent about half of the population in western countries, and the inhibitory function of TIGIT on these cells can be prevented by the anti-TIGIT mAb EOS-448.

EOS-448 induces preferential depletion of Tregs *ex vivo*

Because Tregs showed a higher proportion of TIGIT$^+$ cells and higher number of TIGIT receptors per cell than other immune populations (**Fig. 1C**), we measured the ability of anti-TIGIT mAb to induce direct killing of Tregs through ADCC/antibody-dependent cell-mediated phagocytosis (ADCP) as a second mechanism of action, independent of the prevention of ligand binding. To validate direct

Published OnlineFirst December 4, 2020; DOI: 10.1158/1535-7163.MCT-20-0464

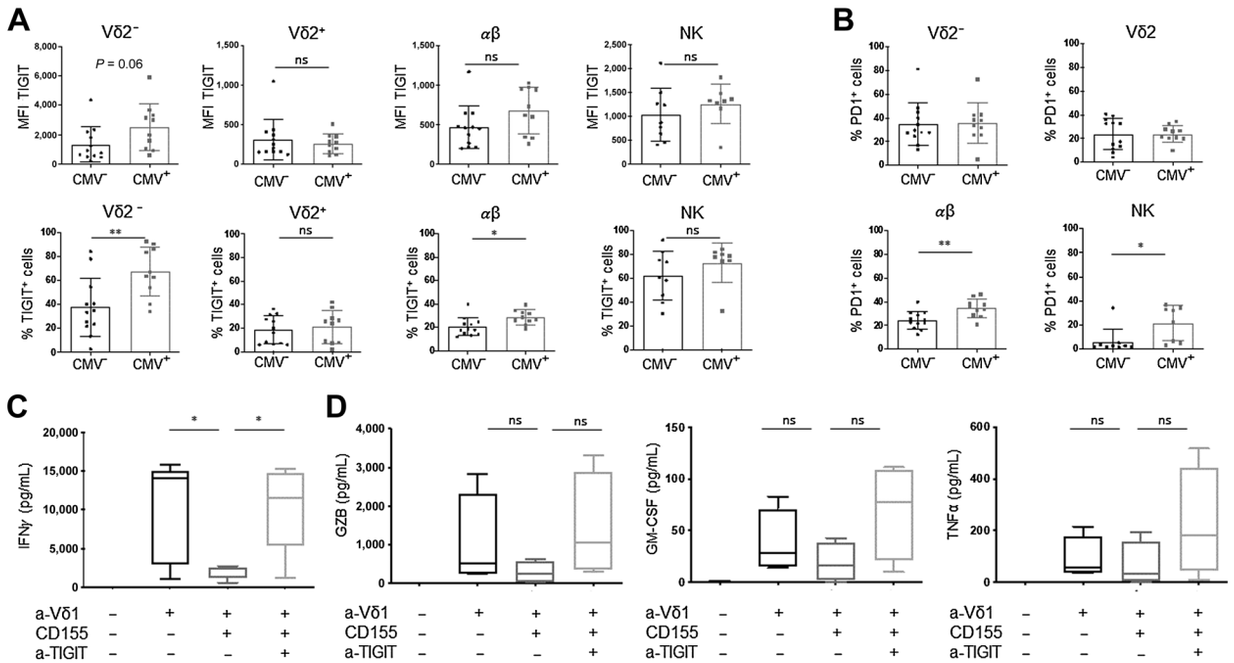

Figure 3.

TIGIT is expressed on γδ T cells and has suppressive activity. **A** and **B,** Flow cytometry analysis for TIGIT (**A**) or PD-1 (**B**) expression in immune populations from CMV-seropositive and negative human volunteers ($n = 22$). **C** and **D,** Vδ2$^-$ T cells were isolated and stimulated *in vitro* by anti-Vδ1 in the presence or absence of CD155 and/or anti-TIGIT mAb EOS-448. Secreted IFNγ (**C**) or other proinflammatory cytokines (**D**) were measured by ELISA ($n = 5$ donors). Data are represented as dot plots and histograms with mean ±SD (**A** and **B**) or Tukey plots (**C** and **D**). *, $P < 0.05$; **, $P < 0.01$ by Student *t* test.

cytotoxic potential, we compared several isotypes of anti-TIGIT Ab (human IgG1, IgG2, and IgG4) and confirmed that only hIgG1 mAb could engage FcγR on effector cells and induce direct cell killing (Supplementary Fig. S5B). We then tested the cytotoxic potential in unmanipulated whole PBMCs from a patient with cancer. There was lytic activity of EOS-448 on Tregs, whereas CD4$^+$ or CD8$^+$ T cells, which are among the non-Treg cells that express the highest level of TIGIT, were significantly less impacted, both for total and memory subsets (**Fig. 4D** and **E**; Supplementary Fig. S5C). A similar assay was performed on samples from seven patients (four different indications) and confirmed the preferred cytotoxic potential against Tregs over non-Treg T-cell populations (**Fig. 4E**), with the exception of one sample from a patient with bladder cancer that demonstrated high cytotoxicity in all populations (**Fig. 4E**). This increased cytotoxic potential toward Tregs correlated with a higher expression of TIGIT receptors per cell (**Fig. 4F**). The populations less sensitive to EOS-448 lytic potential, such as the memory CD8 subset, might thus benefit from the antagonistic EOS-448 activity to restore their functionality.

TIGIT inhibition shows strong antitumor therapeutic activity *in vivo* and depends on mAb isotype and binding to FcγR

Preclinical models using anti-TIGIT mAbs have shown different outcomes; one study showed no single-agent efficacy against CT26 tumors (3), while another demonstrated a potent response (17). To better characterize the potency of a mouse surrogate anti-TIGIT mAb, we conducted experiments in tumor models, such as CT26 and Hepa1–6. These experiments confirmed strong tumor growth delay with some complete responses in both models when anti-TIGIT mAb was built on the mouse IgG2a isotype that effectively engages activatory Fcγ receptors (FcγR; **Fig. 5A** and **B**). In contrast, when the same anti-TIGIT Ab clone was built on a mouse IgG1 isotype, with reduced affinity for activatory FcγR, the antitumor activity was completely lost (**Fig. 5C**). To understand whether the antitumor effect of anti-TIGIT mAb was dependent on engagement of activatory FcγR, we tested the activity of mIgG2a anti-TIGIT mAb in FcγR chain KO mice, which lack surface expression and signaling of all activatory FcγR. Similar to mIgG1 in wild-type animals, anti-TIGIT mIgG2a had no activity in FcRγ chain KO mice (**Fig. 5D**). To further support the importance of FcγR engagement and provide insight into the mechanism of anti-TIGIT Ab therapy, we assessed effects on TILs and observed that antitumor efficacy of anti-TIGIT mIgG2a mAb was correlated with partial depletion of Tregs within the TME (whereas CD8$^+$ T cells and peripheral Tregs were not impacted; **Fig. 5E**; Supplementary Fig. S6A and S6B). These results correlate with a higher TIGIT expression on Tregs within the TME (Supplementary Fig. S6C), as observed in humans (**Figs. 1C** and **D** and **4F**). To investigate which cells were involved in anti-TIGIT mIgG2a antitumor efficacy, we treated CT26 tumors with anti-TIGIT and anti–PD-1 after NK or macrophage depletion. Under these conditions, the antitumor activity of the combination treatment was lost (Supplementary Fig. S6E and S6F). Interestingly, an increase of IFNγ-producing CD4$^+$ and CD8$^+$ T cells within the TME after treatment with anti-TIGIT mIgG2a was also observed (**Fig. 5F**). To determine whether antitumor activity of anti-TIGIT mAb was only dependent on Treg-depleting potential and whether immunomodulation through competition with CD155 ligand was playing any role, we compared the activity of mIgG1 and mIgG2a isotypes of anti-TIGIT Ab on tumors depleted for CD4$^+$ T cells (Tregs represent 50% of total CD4$^+$ T-cell population in CT26 model). Under this condition, anti-TIGIT mIgG1 isotype also demonstrated potent antitumor effect through its ICI activity (Supplementary Fig. S6D).

Published OnlineFirst December 4, 2020; DOI: 10.1158/1535-7163.MCT-20-0464

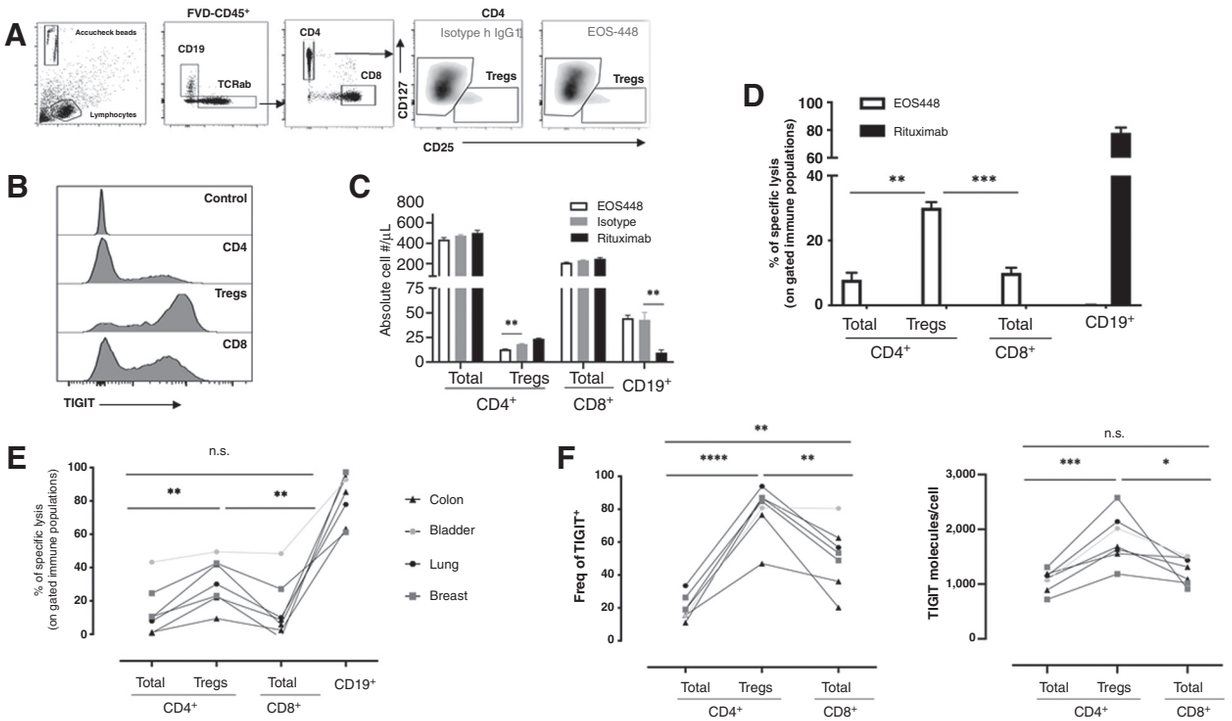

Figure 4.

EOS-448 triggers preferential antibody-dependent lysis of Tregs. **A,** Flow cytometry gating strategy for the lung cancer PBMC sample shown in **B, C,** and **D**. **B,** Expression levels of TIGIT in the untreated wells among the different analyzed populations. **C,** Absolute cell number/µL calculated by FACS, using Accucheck beads for normalization across wells. Normalized counts are shown for $CD4^+$ and $CD8^+$ T cells, Tregs, and $CD19^+$ cell populations from a lung cancer patient PBMCs and incubated *ex vivo* with either EOS-448, isotype control, or rituximab. Results are shown as mean ±SEM from triplicates. **D,** Percent of specific lysis calculated with the absolute cell counts/µL shown in **C**. Results are shown as mean ±SEM from triplicates for conditions treated either with EOS-448 or rituximab, as detailed in the Materials and Methods. **E,** Dot plots showing the mean percent of specific lysis analyzed as shown in **D** on PBMCs from several indications including bladder ($n = 1$), breast ($n = 2$), colon ($n = 3$), and lung ($n = 1$) solid cancers. Results are expressed as mean value of triplicates for each population and populations from the same donor are matched with a line. **F,** Graph showing pooled data analysis of the frequency of $TIGIT^+$ cells (left) and the number of TIGIT molecules per cell (right) in populations from different patients with cancer analyzed in **E**. *, $P < 0.05$; **, $P < 0.01$; ***, $P < 0.001$ by Student *t* test.

Finally, because anti-TIGIT mAb has been described to act synergistically with anti–PD-1 (3) and to further test the combination potential of anti-TIGIT mAb, we combined treatment of anti-TIGIT mAb with Abs targeting costimulatory molecules (i.e., 4-1BB, OX-40, or GITR) in subcutaneous CT26, MC38, and PanO2 models. We observed a strong additive or synergistic effect of the combination treatment that was not limited to anti–PD-1 (**Fig. 5G**; Supplementary Fig. S6G). All mice with a complete response against CT26 developed a long-lasting tumor-specific memory response capable of protecting them against rechallenge with CT26, but not EMT6, tumor cells (Supplementary Fig. S6H).

TIGIT is expressed by specific cancer cells and represents a target for direct cytotoxicity

TIGIT has been described to be specifically expressed on immune cells (1). Following an investigation of public databases for TIGIT gene expression in cancers, we identified a high proportion of hematologic malignancies among indications exhibiting high expression levels (Supplementary Fig. S7). To determine whether this observation was due to strong TIGIT expression by immune cells in these blood cancers or to expression on tumor cells themselves, we acquired fresh samples from patients with Sézary syndrome. To differentiate the normal and tumor $CD4^+$ T-cell population in these samples, we first determined the TCR-Vβ rearrangement corresponding to the tumor clone. TIGIT was stained on both $CD4^+$ populations and the results showed the existence of a $TIGIT^+$ population on the $CD4^+$ tumor cells (**Fig. 6A**). When data from 23 patients were pooled, more than 80% of tumor cells expressed TIGIT in 21 of 23 patients. This finding confirmed a high level of TIGIT expression on tumor cells themselves (**Fig. 6B**), whereas normal circulating $CD4^+$ T cells had moderate TIGIT expression, as observed in other solid tumors (**Fig. 1**).

Because TIGIT was found on the surface of tumor cells, we explored whether anti-TIGIT mAb EOS-448 could have a direct antitumor cytotoxic effect. Fresh blood samples from patients with Sézary syndrome were tested for ADCC potential against different TIGIT-expressing populations using autologous NK effector cells. In three of four patient samples, direct cytotoxicity was observed on tumor $CD4^+$ cells and increased with the E:T ratio. This cytotoxicity was either undetectable or significantly reduced in nonmalignant $CD4^+$ or NK-cell subsets (**Fig. 6C**). To further confirm that anti-TIGIT mAb could demonstrate potential antitumor effects through direct cytotoxicity on tumor cells, we established a mouse model with EL4 T-cell lymphoma that was engineered to express mouse TIGIT. Similar to the results observed in human cancer samples, mouse surrogate anti-TIGIT mAb could trigger lysis of EL4-mTIGIT cells *in vitro* (**Fig. 6D**). We then tested the *in vivo* potential of anti-TIGIT mAb therapy against

Published OnlineFirst December 4, 2020; DOI: 10.1158/1535-7163.MCT-20-0464

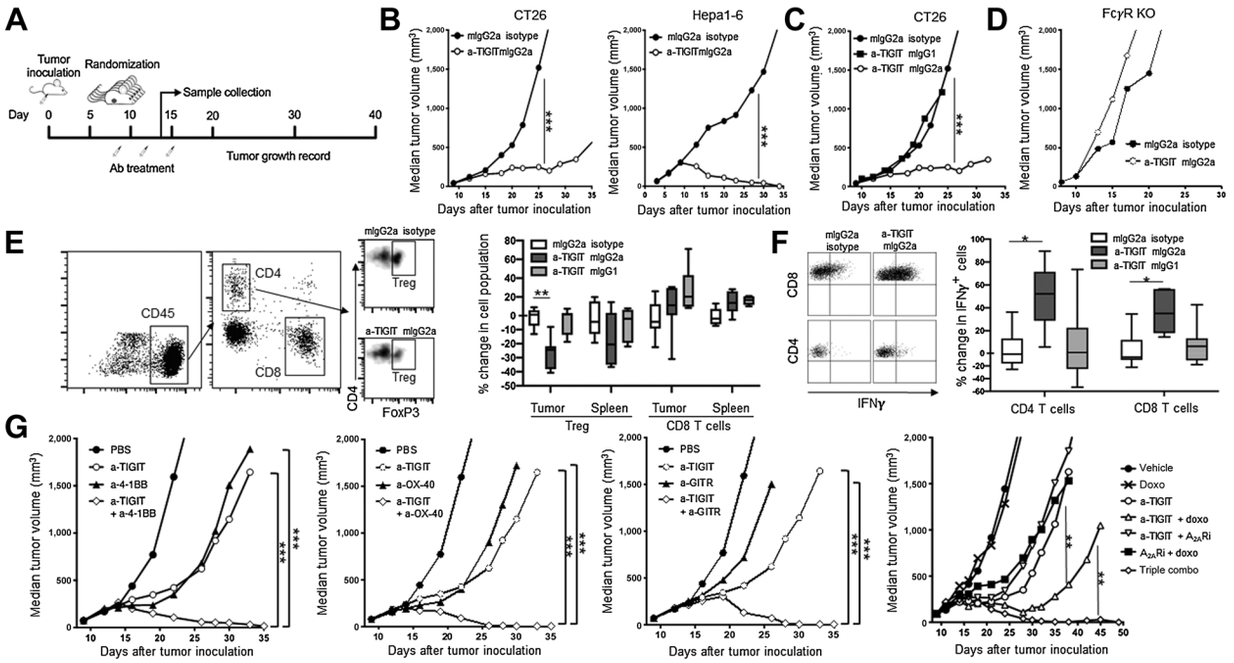

Figure 5.

Anti-TIGIT mIgG2a antibody shows strong antitumor activity *in vivo*. **A,** Schematic representation of *in vivo* experiments performed in **B**. **B,** Median tumor growth curves for mice treated with mIgG2a isotype control or anti-TIGIT mIgG2a in CT26 colon carcinoma or Hepa1–6 hepatocarcinoma mouse models (n = 10 mice/group); graphs are representative of three independent experiments per model. Median tumor growth curves for mice treated with mIgG2a isotype, anti-TIGIT mIgG2a, or anti-TIGIT mIgG1 in CT26 tumor bearing wild-type (**C**) or FcγR chain KO (**D**) mice. Results shown are representative of two independent experiments. **E,** FACS analysis showing percent change in Tregs and $CD8^+$ T-cell populations in CT26 dissociated tumors after *in vivo* treatment with anti-TIGIT mIgG2a, anti-TIGIT mIgG1, or mIgG2a isotype control. **F,** Percent change in IFNγ-producing cells among $CD4^+$ and $CD8^+$ T-cell populations in samples from stimulated *ex vivo* with PMA/ionomycin (**E**). Data in **E** and **F** are represented as Tukey plots normalized to the average of isotype-treated animals (n = 8/group) and are representative of three independent experiments. **G,** Median tumor growth curves for mice treated with PBS, anti-TIGIT mIgG2a, or other immune modulators (as indicated in the legend), as single agent or in combination (n = 10 mice/group). This experiment, performed in CT26 tumor-bearing mice, is representative of three models. Linear mixed model was used for statistical analysis of tumor growth curves. Student t test was used for analysis of Tukey plots. *, $P < 0.05$; **, $P < 0.01$; ***, $P < 0.001$ versus isotype or PBS-treated group.

established EL4 tumors and showed that anti-TIGIT mAb therapy is active in EL4-expressing TIGIT, but not in control EL4 cells expressing GFP (**Fig. 6E**). Finally, the single amino acid mutation N297A in anti-TIGIT mAb that decreases affinity to FcγR completely abolished its therapeutic potential and confirmed the FcγR-mediated mechanism of action in this setting (**Fig. 6E**). To the best of our knowledge, this is the first report to show the direct anticancer potential of an anti-TIGIT mAb therapy, not only by preventing immunosuppression through TIGIT blockade and depletion of Treg cells, but also by a third mechanism of action linked to its direct cytotoxicity on TIGIT-expressing tumor cells.

Discussion

Cancer immunotherapy with ICIs has demonstrated long-term responses in a large number of patients with cancer as proof of concept of the potential to harness the immune system to fight cancer. Three ICI drugs have been approved (anti-CTLA-4, anti–PD-1, and anti–PD-L1) in multiple indications, but durable responses are still limited to a minority of patients and drug resistance or toxicity or both are frequently observed (29, 30).

Although many new drugs targeting numerous ICIs have been developed in recent years, none so far has demonstrated significant clinical activity (as a single agent or in combination) in a randomized study, with the unique exception of the anti-TIGIT Ab tiragolumab. Recently released data from a randomized phase II trial showed a significant benefit of tiragolumab in NSCLC when combined with an a–PD-L1 drug, leading to initiation of multiple pivotal studies (31).

On the basis of the observation that TIGIT appears as the most promising ICI in the post–PD-1 era, there is a strong and urgent need to understand why anti-TIGIT drugs demonstrate significant clinical efficacy and whether all anti-TIGIT Abs have similar therapeutic potential. Our data using EOS-448, a clinical stage hIgG1 anti-TIGIT mAb, demonstrate an important competitive advantage for anti-TIGIT drugs, with FcγR engagement capacity that is linked to important depleting potential on Treg as well as on tumor cells. In parallel, anti-TIGIT mAbs show multiple mechanisms of action linked to restoration of functional activity of multiple T-cell populations.

In particular, we demonstrated that TIGIT expression was not restricted to αβ T cells, but was also observed at high levels on nonconventional γδ T cells. Because γδ T cells have been identified as the most favorable cancer-wide prognostic signature for outcome and have been shown to play an antitumor role (32, 33), we explored the possible mechanistic function of the CD155–TIGIT axis in that immune cell population. Similar to αβ T cells, we confirmed that γδ T cells express TIGIT and are sensitive to CD155-mediated immunosuppression that is fully prevented by anti-TIGIT mAb EOS-448. Although previous reports demonstrated the low expression and

Published OnlineFirst December 4, 2020; DOI: 10.1158/1535-7163.MCT-20-0464

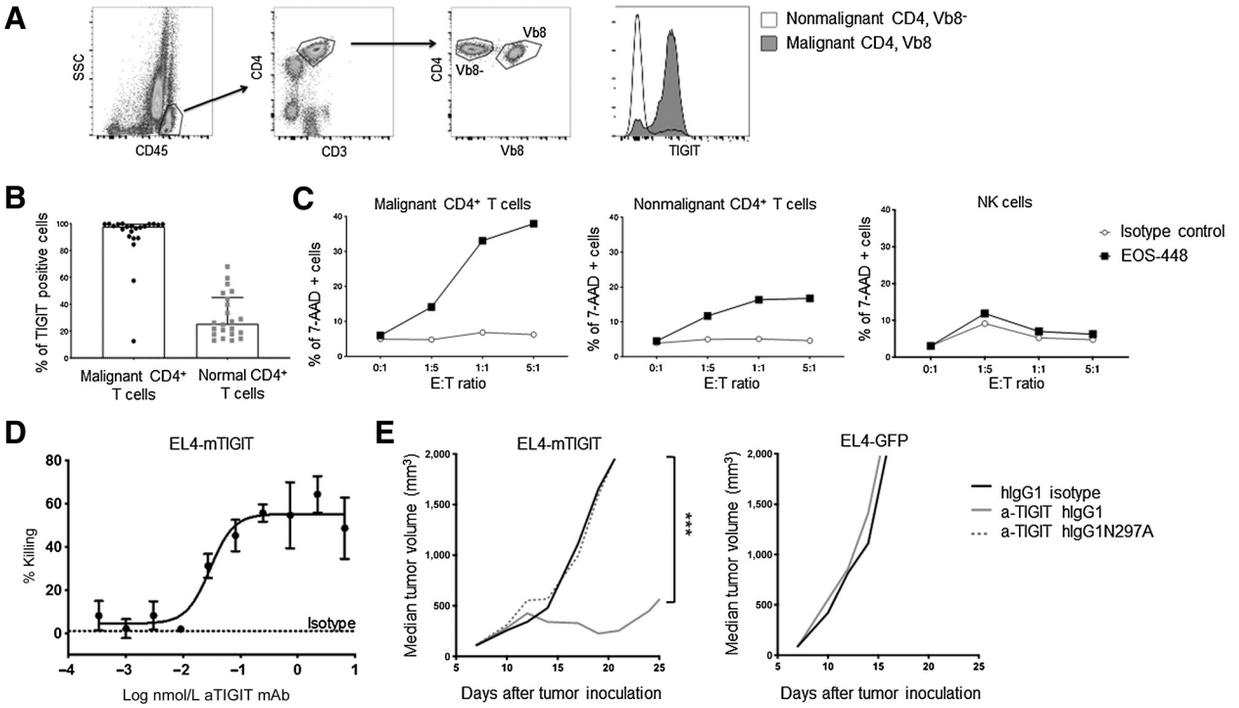

Figure 6.

TIGIT is expressed on tumor cells and represents a target for ADCC. **A,** Flow cytometry showing gating strategy and TIGIT expression on malignant (TCRVb$^+$ CD3$^+$ CD4$^+$) and nonmalignant (TCRVb$^-$ CD3$^+$ CD4$^+$) cells. **B,** Dot plots and median percentage from FACS analysis of TIGIT$^+$ cells among malignant versus nonmalignant CD4$^+$ T cells ($n = 23$ patients). **C,** Cell death monitored through the incorporation of 7-AAD of the malignant CD4$^+$ T cells, nonmalignant CD4$^+$ T cells, and NK cells in the presence of isotype control or anti-TIGIT mAb EOS-448. Results are shown for one representative donor out of four and are expressed as the percent of 7-AAD$^+$ cells among each population at a given E:T ratio. **D,** Dose response curve for anti-TIGIT–dependent lysis of murine EL4-mTIGIT cells in the presence of Raw264.7 effector cells in a 5:1 E/T ratio. Data are represented as percent of target cell killing normalized to isotype control. **E,** Median tumor growth curves for EL4-mTIGIT (left) and EL4-GFP (right) tumors treated with hIgG1 isotype, anti-TIGIT hIgG1, or anti-TIGIT hIgG1-N297A ($n = 10$ mice/group). ***, $P < 0.001$ versus isotype-treated group.

limited mechanistic function of PD-1 and TIGIT in the Vδ2 subpopulation of γδ T cells (34, 35), our data suggest that other γδ T-cell subpopulations, such as Vδ1 cells, express TIGIT and are sensitive to TIGIT-mediated immunosuppression. Although such activity had been observed in αβ T cells and NK cells, to our knowledge, this is the first study to demonstrate that TIGIT can mediate suppressive activity on γδ T cells. This finding could have important implications regarding the mechanism by which tumors induce immunosuppression, either by suppressing γδ T-cell functionality or polarizing them toward a Treg phenotype (35, 36). To further confirm the relevance of our finding in a disease setting, additional work is needed to specifically examine the effect of TIGIT on γδ T cells in the clinic or in animal tumor models.

In addition, among different T-cell populations, we observed a higher proportion of TIGIT$^+$ cells in TME compared with PBMCs from patients with cancer and healthy volunteers, which was similar to previous reports that showed increased TIGIT expression in the TME (3, 12, 14). Furthermore, the proportion of tumor-infiltrating Tregs that express TIGIT was close to 100%, which is in agreement with data comparing the expression of different immune checkpoints in Tregs (37). While comparing the density of TIGIT molecules, we noticed that the highest expression was specifically on infiltrating Tregs, potentially labeling them as ideal targets for ADCC/ADCP. We confirmed preferential Treg depletion, which could be explained by either the higher expression level (**Figs. 1D** and **4F**; Supplementary Fig. S6C) or by a different cell-intrinsic mechanism with higher susceptibility of Tregs to ADCC/ADCP–mediated lysis (as has been observed for other mAbs targeting GITR, CTLA-4, or 4-1BB; refs. 38–40). This novel role of an anti-TIGIT mAb holds potential because Tregs in the TME, and particularly TIGIT$^+$ Tregs that form a functionally distinct Treg subset, are known to play a strong immunosuppressive role and are associated with poor outcome in several cancer indications (2, 41). Interestingly, recent data showed no NK cell–mediated killing of activated TIGIT$^+$ CD8$^+$ T cells with a regular hIgG1 anti-TIGIT, as opposed to an isotype with enhanced effector function (42), further supporting the selection of an hIgG1 format to preferentially target Tregs while preserving most TIGIT$^+$ effector cells. In addition, an anti-TIGIT hIgG1 has been shown to be very safe for patients, as a single agent or in combination with a–PD-(L)1, as has been reported for the CITYSCAPE trial (31).

Our data comparing therapeutic activity in the mouse tumor models clearly demonstrate the superior activity of anti-TIGIT mAbs with an isotype engaging activatory FcγR that correlates with preferred Treg depletion and increased intratumor CD8:Treg ratio. Our data confirm findings showing strong therapeutic efficacy of anti-TIGIT mAbs with an ADCC/ADCP–enabled isotype (43, 44), unlike those reported by Johnston and colleagues (3) showing no single-agent efficacy. The Treg depletion observed in our model might be explained by the higher affinity of the surrogate anti-TIGIT mAb used in our study compared with clone 10A7 used in previous studies (3, 44). Overall, these results

Published OnlineFirst December 4, 2020; DOI: 10.1158/1535-7163.MCT-20-0464

strongly suggest the higher therapeutic potential of anti-TIGIT mAbs with high affinity for activatory FcγR over FcγR-disabled isotypes in clinical studies.

To further characterize TIGIT expression in cancer, we compared several gene expression databases for TIGIT expression and found the highest level of TIGIT in hematologic malignancies, particularly in T-cell lymphoma. To understand whether this observation could be linked to either strong TIGIT expression on nontumoral immune populations or direct expression by cancer cells, we examined the presence of TIGIT in samples from patients with Sézary syndrome. As expected, we observed moderate TIGIT expression on the membrane of nonmalignant T cells, but, more surprisingly, we also confirmed the presence of TIGIT on nearly all malignant cells in most patients. Although strong TIGIT expression had been reported in $CD4^+$ T-cell populations in Sézary syndrome samples (13), no distinction was made between normal or malignant cells. Taking advantage of this observation, we explored the potential of EOS-448 for direct cytotoxicity of tumor cells, as has been observed for molecules like rituximab and trastuzumab (45, 46), in fresh samples from patients with Sézary syndrome. The results demonstrated a clear cytotoxic activity of EOS-448 against TIGIT-expressing $CD4^+$ tumor cells, whereas normal $CD4^+$ T cells and NK cells that express TIGIT were not affected or were only mildly affected. We also tested this hypothesis *in vivo* in mice using engineered tumor cells expressing mTIGIT (as opposed to observations in humans, we could not identify murine tumor cells naturally expressing TIGIT), and showed that anti-TIGIT Ab had strong therapeutic efficacy that directly depended on antibody isotype and TIGIT expression by tumor cells. These results reveal a novel mechanism of action of anti-TIGIT Abs, that being a direct cytotoxic effect against tumor cells. As we have previously reported TIGIT expression on tumor cells in lymphoma indications from B-cell origin such as CLL (47), this finding represents an additional opportunity for anti-TIGIT agents in blood cancers, which should be further explored.

Overall, our data reveal new perspectives for the use of anti-TIGIT Abs in the clinic that, based on previous and current work, could rely on a few proinflammatory effects to further benefit patients. In particular, our data provide strong rationale for the selection of an anti-TIGIT mAb with an FcγR-engaging isotype that could act by inducing (i) reversion of NK and T-cell (including γδ T cells) dysfunction linked with cancer progression; (ii) engagement of FcγR and preferential depletion of intratumoral Tregs expressing high levels of TIGIT; and (iii) direct cytotoxic activity of tumor cells in specific hematologic malignancies. Interestingly, several trials are currently testing the anti-TIGIT mAb format (47), with the hIgG1 isotype (like tiragolumab, which has demonstrated clinical benefit; ref. 31) being the most promising format, and clinical data are now needed to understand which mechanism(s) will prevail.

Authors' Disclosures

J. Cuende reports a patent for WO/2020/144178 pending and issued and WO/2019/023504 pending and issued. A. Pappalardo reports grants from iTeos Therapeutics during the conduct of the study. S. Denies reports a patent for WO2019023504A1 pending. V. Pitard reports grants from Iteos during the conduct of the study. M. Bagot reports non-financial support from Innate Pharma, personal fees from Kyowa Kirin, Galderma, Takeda, and Helsinn/Recordati outside the submitted work. F. Lambolez reports a patent for WO/2020/144178 pending and issued and WO/2019/023504 pending and issued. M.J. Carter reports grants from iTeos during the conduct of the study. M. Cragg reports grants from iTeos during the conduct of the study, personal fees from Bioinvent, grants from GSK and Bioinvent outside the submitted work. J. Déchanet-Merville reports grants from iTeos Therapeutics during the conduct of the study. G. Driessens reports a patent for WO/2019/023504 pending and issued and WO/2020/144178 pending and issued. C. Hoofd reports a patent for 35041-42519/US pending and issued. No disclosures were reported by the other authors.

Authors' Contributions

J. Preillon: Resources, formal analysis, investigation, methodology, writing-original draft, writing-review and editing. **J. Cuende:** Conceptualization, resources, formal analysis, investigation, writing-original draft, writing-review and editing. **V. Rabolli:** Resources, formal analysis, investigation, writing-original draft. **L. Garnero:** Resources. **M. Mercier:** Resources, formal analysis, investigation, writing-original draft. **N. Wald:** Resources, formal analysis, investigation, writing-original draft. **A. Pappalardo:** Resources, investigation, methodology. **S. Denies:** Conceptualization, formal analysis, investigation. **D. Jamart:** Resources. **A.-C. Michaux:** Resources. **R. Pirson:** Resources, investigation. **V. Pitard:** Resources, investigation. **M. Bagot:** Supervision. **S. Prasad:** Resources, investigation. **E. Houthuys:** Resources, formal analysis. **M. Brouwer:** Resources. **R. Marillier:** Resources, formal analysis, supervision. **F. Lambolez:** Conceptualization, resources, formal analysis, investigation. **J.R. Marchante:** Resources, software, formal analysis, writing-original draft. **F. Nyawouame:** Resources. **M.J. Carter:** Resources, formal analysis, investigation. **V. Baron-Bodo:** Resources, formal analysis, supervision. **A. Marie-Cardine:** Resources, investigation, methodology. **M. Cragg:** Conceptualization, supervision. **J. Déchanet -Merville:** Conceptualization, supervision. **G. Driessens:** Conceptualization, formal analysis, supervision, validation, investigation, methodology, writing-original draft, writing-review and editing. **C. Hoofd:** Conceptualization, resources, formal analysis, supervision, investigation, writing-original draft, writing-review and editing.

Acknowledgments

Editorial support was provided by Cindy Taylor, Synterex, Inc.

Received June 5, 2020; revised August 24, 2020; accepted November 3, 2020; published first December 4, 2020.

References

1. Yu X, Harden K, Gonzalez LC, Francesco M, Chiang E, Irving B, et al. The surface protein TIGIT suppresses T cell activation by promoting the generation of mature immunoregulatory dendritic cells. Nat Immunol 2009;10:48–57.
2. Joller N, Lozano E, Burkett PR, Patel B, Xiao S, Zhu C, et al. Treg cells expressing the coinhibitory molecule TIGIT selectively inhibit proinflammatory Th1 and Th17 cell responses. Immunity 2014;40:569–81.
3. Johnston RJ, Comps-Agrar L, Hackney J, Yu X, Huseni M, Yang Y, et al. The immunoreceptor TIGIT regulates antitumor and antiviral CD8(+) T cell effector function. Cancer Cell 2014;26:923–37.
4. Lucca LE, Axisa PP, Singer ER, Nolan NM, Dominguez-Villar M, Hafler DA. TIGIT signaling restores suppressor function of Th1 Tregs. JCI Insight 2019;4:e124427.
5. Levin SD, Taft DW, Brandt CS, Bucher C, Howard ED, Chadwick EM, et al. Vstm3 is a member of the CD28 family and an important modulator of T-cell function. Eur J Immunol 2011;41:902–15.
6. Lozano E, Dominguez-Villar M, Kuchroo V, Hafler DA. The TIGIT/CD226 axis regulates human T cell function. J Immunol 2012;188:3869–75.
7. Pauken KE, Wherry EJ. TIGIT and CD226: tipping the balance between costimulatory and coinhibitory molecules to augment the cancer immunotherapy toolkit. Cancer Cell 2014;26:785–7.
8. Manieri NA, Chiang EY, Grogan JL. TIGIT: A key inhibitor of the cancer immunity cycle. Trends Immunol 2017;38:20–8.
9. Chew GM, Fujita T, Webb GM, Burwitz BJ, Wu HL, Reed JS, et al. TIGIT marks exhausted T Cells, correlates with disease progression, and serves as a target for immune restoration in HIV and SIV infection. PLoS Pathog 2016;12:e1005349.

10. Fuhrman CA, Yeh WI, Seay HR, Saikumar Lakshmi P, Chopra G, Zhang L, et al. Divergent phenotypes of human regulatory T cells expressing the receptors TIGIT and CD226. J Immunol 2015;195:145–55.
11. Kurtulus S, Sakuishi K, Ngiow SF, Joller N, Tan DJ, Teng MW, et al. TIGIT predominantly regulates the immune response via regulatory T cells. J Clin Invest 2015;125:4053–62.
12. Zheng C, Zheng L, Yoo JK, Guo H, Zhang Y, Guo X, et al. Landscape of infiltrating T cells in liver cancer revealed by single-cell sequencing. Cell 2017; 169:1342–56.
13. Jariwala N, Benoit B, Kossenkov AV, Oetjen LK, Whelan TM, Cornejo CM, et al. TIGIT and Helios are highly expressed on CD4(+) T cells in Sezary syndrome patients. J Invest Dermatol 2017;137:257–60.
14. Harjunpää H, Guillerey C. TIGIT as an emerging immune checkpoint. Clin Exp Immunol 2020;200:108–19.
15. Li X, Wang R, Fan P, Yao X, Qin L, Peng Y, et al. A comprehensive analysis of key immune checkpoint receptors on tumor-infiltrating T cells from multiple types of cancer. Front Oncol 2019;9:1066.
16. Solomon BL, Garrido-Laguna I. TIGIT: a novel immunotherapy target moving from bench to bedside. Cancer Immunol Immunother 2018;67:1659–67.
17. Zhang Q, Bi J, Zheng X, Chen Y, Wang H, Wu W, et al. Blockade of the checkpoint receptor TIGIT prevents NK cell exhaustion and elicits potent anti-tumor immunity. Nat Immunol 2018;19:723–32.
18. Hung AL, Maxwell R, Theodros D, Belcaid Z, Mathios D, Luksik AS, et al. TIGIT and PD-1 dual checkpoint blockade enhances antitumor immunity and survival in GBM. Oncoimmunology 2018;7:e1466769.
19. Guillerey C, Harjunpaa H, Carrie N, Kassem S, Teo T, Miles K, et al. TIGIT immune checkpoint blockade restores CD8(+) T cell immunity against multiple myeloma. Blood 2018;132:1689–94.
20. Dixon KO, Schorer M, Nevin J, Etminan Y, Amoozgar Z, Kondo T, et al. Functional anti-TIGIT antibodies regulate development of autoimmunity and antitumor immunity. J Immunol 2018;200:3000–7.
21. Minnie SA, Kuns RD, Gartlan KH, Zhang P, Wilkinson AN, Samson L, et al. Myeloma escape after stem cell transplantation is a consequence of T-cell exhaustion and is prevented by TIGIT blockade. Blood 2018;132:1675–88.
22. Chauvin JM, Pagliano O, Fourcade J, Sun Z, Wang H, Sander C, et al. TIGIT and PD-1 impair tumor antigen-specific CD8(+) T cells in melanoma patients. J Clin Invest 2015;125:2046–58.
23. Sanchez-Correa B, Valhondo I, Hassouneh F, Lopez-Sejas N, Pera A, Bergua JM, et al. DNAM-1 and the TIGIT/PVRIG/TACTILE axis: novel immune checkpoints for natural killer cell-based cancer immunotherapy. Cancers 2019;11:877.
24. Gomes B, Driessens G, Bartlett D, Cai D, Cauwenberghs S, Crosignani S, et al. Characterization of the selective indoleamine 2,3-dioxygenase-1 (IDO1) catalytic inhibitor EOS200271/PF-06840003 supports IDO1 as a critical resistance mechanism to PD-(L)1 blockade therapy. Mol Cancer Ther 2018;17:2530–42.
25. Beers SA, French RR, Chan HT, Lim SH, Jarrett TC, Vidal RM, et al. Antigenic modulation limits the efficacy of anti-CD20 antibodies: implications for antibody selection. Blood 2010;115:5191–201.
26. Marie-Cardine A, Viaud N, Thonnart N, Joly R, Chanteux S, Gauthier L, et al. IPH4102, a humanized KIR3DL2 antibody with potent activity against cutaneous T-cell lymphoma. Cancer Res 2014;74:6060–70.
27. Liu C, Cripe TP, Kim MO. Statistical issues in longitudinal data analysis for treatment efficacy studies in the biomedical sciences. Mol Ther 2010;18:1724–30.
28. Couzi L PV, Moreau JF, Merville P, Déchanet-Merville J. Direct and indirect effects of cytomegalovirus-induced γδ T cells after kidney transplantation. Front Immunol 2015;6:3.
29. Seidel JA, Otsuka A, Kabashima K. Anti-PD-1 and anti-CTLA-4 therapies in cancer: mechanisms of action, efficacy, and limitations. Front Oncol 2018;8:86.
30. Restifo NP, Smyth MJ, Snyder A. Acquired resistance to immunotherapy and future challenges. Nat Rev Cancer 2016;16:121–6.
31. Rodriguez-Abreu D, Johnson ML, Hussein MA, Cobo M, Patel AJ, Secen NM, et al. Primary analysis of a randomized, double-blind, phase II study of the anti-TIGIT antibody tiragolumab (tira) plus atezolizumab (atezo) versus placebo plus atezo as first-line (1L) treatment in patients with PD-L1-selected NSCLC (CITYSCAPE). J Clin Oncol 2020;38:9503-.
32. Gentles AJ NA, Liu CL, Bratman SV, Feng W, Kim D, et al. The prognostic landscape of genes and infiltrating immune cells across human cancers. Nat Med 2015;21:938–45.
33. Meraviglia S, Lo Presti E, Tosolini M, La Mendola C, Orlando V, Todaro M, et al. Distinctive features of tumor-infiltrating γδ T lymphocytes in human colorectal cancer. Oncoimmunology 2017;6:e1347742.
34. Zumwalde NA, Sharma A, Xu X, Ma S, Schneider CL, Romero-Masters JC, et al. Adoptively transferred Vγ9Vδ2 T cells show potent antitumor effects in a preclinical B cell lymphomagenesis model. JCI Insight 2017;2:e93179.
35. Lo Presti E, Pizzolato G, Corsale AM, Caccamo N, Sireci G, Dieli F, et al. γδ T cells and tumor microenvironment: from immunosurveillance to tumor evasion. Front Immunol 2018;9:1395.
36. Silva-Santos B, Serre K, Norell H. γδ T cells in cancer. Nat Rev Immunol 2015;15: 683–91.
37. Kim HR, Park HJ, Son J, Lee JG, Chung KY, Cho NH, et al. Tumor microenvironment dictates regulatory T cell phenotype: upregulated immune checkpoints reinforce suppressive function. J Immunother Cancer 2019;7:339.
38. Schoenhals JE, Cushman TR, Barsoumian HB, Li A, Cadena AP, Niknam S, et al. Anti-glucocorticoid-induced tumor necrosis factor-related protein (GITR) therapy overcomes radiation-induced Treg immunosuppression and drives abscopal effects. Front Immunol 2018;9:2170.
39. Arce Vargas F, Furness AJS, Litchfield K, Joshi K, Rosenthal R, Ghorani E, et al. Fc effector function contributes to the activity of human anti-CTLA-4 antibodies. Cancer Cell 2018;33:649–63.
40. Buchan SL, Dou L, Remer M, Booth SG, Dunn SN, Lai C, et al. Antibodies to costimulatory receptor 4-1BB enhance anti-tumor immunity via T regulatory cell depletion and promotion of CD8 T cell effector function. Immunity 2018;49: 958–70.
41. Shang B, Liu Y, Jiang SJ, Liu Y. Prognostic value of tumor-infiltrating FoxP3+ regulatory T cells in cancers: a systematic review and meta-analysis. Sci Rep 2015; 5:15179.
42. Lopez A, Tan J, Anderson AE, Udyavar A, Narasappa N, Lee S, et al. Characterization of AB154, a humanized, non-depleting α-TIGIT antibody undergoing clinical evaluation in subjects with advanced solid tumors (P260). J Immunother Cancer 2019;7:282.
43. Argast GM, Cancilla B, Cattaruzza F, Yeung P, Scolan EL, Harris R, et al. Anti-TIGIT biomarker study: inhibition of TIGIT induces loss of Tregs from tumors and requires effector function for tumor growth inhibition. In: Proceedings of the American Association for Cancer Research Annual Meeting 2018; 2018 Apr 14–18; Chicago, IL. Philadelphia (PA): AACR; Abstract nr 5627.
44. Waight JD, Chand D, Dietrich S, Gombos R, Horn T, Gonzalez AM, et al. Selective FcγR co-engagement on APCs modulates the activity of therapeutic antibodies targeting T cell antigens. Cancer Cell 2018;33:1033–47.
45. Hudis CA. Trastuzumab–mechanism of action and use in clinical practice. N Engl J Med 2007;357:39–51.
46. Salles G, Barrett M, Foa R, Maurer J, O'Brien S, Valente N, et al. Rituximab in B-cell hematologic malignancies: a review of 20 years of clinical experience. Adv Ther 2017;34:2232–73.
47. Arruga F, Guerra G, Baev D, Hoofd C, Coscia M, D'Arena GF, et al. Expression of the Tigit/CD226/CD155 receptors/ligand system in chronic lymphocytic leukemia. Blood 2019;134:5454.

AACR American Association for Cancer Research

Molecular Cancer Therapeutics

Restoration of T-cell Effector Function, Depletion of Tregs, and Direct Killing of Tumor Cells: The Multiple Mechanisms of Action of a-TIGIT Antagonist Antibodies

Julie Preillon, Julia Cuende, Virginie Rabolli, et al.

Mol Cancer Ther 2021;20:121-131. Published OnlineFirst December 4, 2020.